Quantifying and reducing spin contamination in algebraic diagrammatic construction theory of charged excitations

Cite as: J. Chem. Phys. **157**, 044106 (2022); https://doi.org/10.1063/5.0097333 Submitted: 27 April 2022 • Accepted: 04 July 2022 • Accepted Manuscript Online: 04 July 2022 • Published Online: 01 August 2022









ARTICLES YOU MAY BE INTERESTED IN

Recent developments in the PySCF program package

The Journal of Chemical Physics 153, 024109 (2020); https://doi.org/10.1063/5.0006074

Unphysical discontinuities, intruder states and regularization in GW methods
The Journal of Chemical Physics 156, 231101 (2022); https://doi.org/10.1063/5.0089317

Dyson-orbital concepts for description of electrons in molecules

The Journal of Chemical Physics 153, 070902 (2020); https://doi.org/10.1063/5.0016472

AIP Publishing The Journal of Chemical Physics Special Topics Open for Submissions

Quantifying and reducing spin contamination in algebraic diagrammatic construction theory of charged excitations

Cite as: J. Chem. Phys. 157, 044106 (2022); doi: 10.1063/5.0097333

Submitted: 27 April 2022 • Accepted: 4 July 2022 •

Published Online: 1 August 2022











Terrence L. Stahl, D Samragni Banerjee, D and Alexander Yu. Sokolov D



AFFILIATIONS

Department of Chemistry and Biochemistry, The Ohio State University, Columbus, Ohio 43210, USA

a) Author to whom correspondence should be addressed: sokolov.8@osu.edu

ABSTRACT

Algebraic diagrammatic construction (ADC) theory is a computationally efficient and accurate approach for simulating electronic excitations in chemical systems. However, for the simulations of excited states in molecules with unpaired electrons, the performance of ADC methods can be affected by the spin contamination in unrestricted Hartree-Fock (UHF) reference wavefunctions. In this work, we benchmark the accuracy of ADC methods for electron attachment and ionization of open-shell molecules with the UHF reference orbitals (EA/IP-ADC/UHF) and develop an approach to quantify the spin contamination in charged excited states. Following this assessment, we demonstrate that the spin contamination can be reduced by combining EA/IP-ADC with the reference orbitals from restricted open-shell Hartree-Fock (ROHF) or orbital-optimized Møller-Plesset perturbation (OMP) theories. Our numerical results demonstrate that for open-shell systems with strong spin contamination in the UHF reference, the third-order EA/IP-ADC methods with the ROHF or OMP reference orbitals are similar in accuracy to equation-of-motion coupled cluster theory with single and double excitations.

Published under an exclusive license by AIP Publishing. https://doi.org/10.1063/5.0097333

I. INTRODUCTION

Charged excitations are an important class of light-matter interactions that result in a generation of free charge carriers (electrons or holes) in a chemical system. Theoretical simulations of charged excitations find applications in determining the redox properties of molecules, understanding the electronic structure of materials, interpreting the photoelectron spectra, and elucidating the mechanisms of photoredox catalytic reactions and genetic damage of biomolecules. 1-7 However, accurate modeling of charged excitations is very challenging as it requires an accurate description of electron correlation, orbital relaxation, and charge localization

Of particular interest are charged excitations of open-shell molecules with unpaired electrons in the ground electronic state. These excitations are common in atmospheric and combustion chemistry⁸⁻¹³ and are also key to many important reactions in organic synthesis. 11,14-18 Simulating charged excitations in openshell molecules presents new challenges, such as an accurate description of electronic spin states and an increased importance of electron correlation effects. In particular, an inadequate description of electronic spin in the ground or charged excited states can lead to spin contamination that can significantly affect the performance of approximate electronic structure theories. Spin contamination can be mitigated using a variety of theoretical approaches, including coupled cluster theory (in its state-specific 19,20 or equation-offormulation), orbital-optimized methods, 26-37 tireference theories.38 A common problem of these approaches is a high computational cost that limits their applicability to small open-shell molecules.

An attractive alternative to conventional electronic structure methods for simulating excited states is algebraic diagrammatic construction theory (ADC). 52-56 ADC offers a framework of computationally efficient and accurate approximations that can compute many excited states incorporating the description of electron correlation effects in a single calculation. Although the ADC methods for charged excited states have been formulated several decades their development and efficient computer implementation have received a renewed interest recently. 60-68 In particular, the non-Dyson ADC methods^{58,59,62,63} allow for independent calculations of electron-attached and ionized excited states with accuracy similar to that of coupled cluster theory with single and double excitations (CCSD)^{19,20} but at a fraction of its computational cost. However, the applications of ADC methods for charged excitations have been primarily limited to closed-shell molecules, with questions remaining about their accuracy for systems with unpaired electrons in the ground electronic state. ^{52,63,68} As a finite-order perturbation theory, ADC is expected to be more sensitive to spin contamination than coupled cluster theory and, thus, may be less accurate when the errors in electronic spin become significant. However, a thorough study of spin contamination in the ADC calculations of charged excitations has not been reported.

In this work, we develop an approach to quantify the spin contamination in ADC calculations of charged excited states of open-shell molecules and investigate how the errors in describing the electronic spin affect the performance of ADC methods. We further demonstrate that the errors in charged excitation energies and spin contamination can be reduced by combining the ADC methods with the reference orbitals from restricted open-shell Hartree–Fock (ROHF)⁶⁹ or nth-order orbital-optimized Møller–Plesset perturbation $[OMP(n)]^{30-34,70-73}$ theories. The resulting theoretical approaches are shown to have similar accuracy to equation-of-motion CCSD (EOM-CCSD) for open-shell molecules with strong spin contamination in the unrestricted Hartree–Fock (UHF) reference wavefunction.

II. THEORY

A. Algebraic diagrammatic construction theory

The central mathematical object in algebraic diagrammatic construction theory of charged excitations is the one-particle Green's function (1-GF, also known as the electron propagator) that contains information about electron affinities (EAs) and ionization energies (IP) of a many-electron system. ^{74–76} In its spectral (Lehmann) representation, 1-GF is defined as

$$G_{pq}(\omega) = \sum_{n} \frac{\langle \Psi_{0}^{N} | a_{p} | \Psi_{n}^{N+1} \rangle \langle \Psi_{n}^{N+1} | a_{q}^{\dagger} | \Psi_{0}^{N} \rangle}{\omega - E_{n}^{N+1} + E_{0}^{N}}$$

$$+ \sum_{n} \frac{\langle \Psi_{0}^{N} | a_{q}^{\dagger} | \Psi_{n}^{N-1} \rangle \langle \Psi_{n}^{N-1} | a_{p} | \Psi_{0}^{N} \rangle}{\omega + E_{n}^{N-1} - E_{0}^{N}}$$

$$= G_{+pq}(\omega) + G_{-pq}(\omega), \qquad (1)$$

where p,q index the molecular orbitals of the system, ω is a complex frequency ($\omega \equiv \omega' + i\eta$), and $G_{+pq}(\omega)$ and $G_{-pq}(\omega)$ are the forward (EA) and backward (IP) components of the propagator, respectively. In Eq. (1), $|\Psi_0^N\rangle$ is the N-electron ground-state wavefunction with energy E_0^N , while $|\Psi_n^{N+1}\rangle$ and $|\Psi_n^{N-1}\rangle$ are the (N+1)- and (N-1)-electron excited states with energies E_n^{N+1} and E_n^{N-1} , respectively. In Eq. (1), the numerators containing the expectation values of creation (a_p^\dagger) and destruction (a_p) operators (so-called residues) describe the probability of EA and IP transitions with energies $\omega_{+n} = E_n^{N+1} - E_0^N$ and $\omega_{-n} = E_0^N - E_n^{N-1}$, respectively.

Equation (1) can be rewritten in a matrix form for each component of 1-GF individually,

$$\mathbf{G}_{\pm}(\omega) = \tilde{\mathbf{X}}_{\pm}(\omega \mathbf{1} - \tilde{\mathbf{\Omega}}_{\pm})^{-1} \tilde{\mathbf{X}}_{\pm}^{\dagger}, \tag{2}$$

where the diagonal matrix $\tilde{\Omega}_{\pm}$ contains the transition energies $\tilde{\Omega}_{\pm nm} = \omega_{\pm n}\delta_{nm}$ and $\tilde{\mathbf{X}}_{\pm}$ is the matrix of spectroscopic (or transition) amplitudes with elements $\tilde{X}_{+pn} = \langle \Psi^0_0 | a_p | \Psi^{N+1}_n \rangle$ or $\tilde{X}_{-qn} = \langle \Psi^0_0 | a_q^\dagger | \Psi^{N-1}_n \rangle$. Equation (2) provides a prescription for calculating 1-GF but is rarely used in practice since the exact (i.e., full configuration interaction) eigenstates $|\Psi^{N\pm1}_n\rangle$ and excitation energies $\omega_{\pm n}$ are prohibitively expensive to compute for realistic systems and basis sets.

Algebraic diagrammatic construction theory (ADC)^{52–56} provides a computationally efficient approach to circumvent this problem by approximating the forward and backward components of the propagator independently of each other using perturbation theory (so-called non-Dyson approach).^{58,59,62,63} ADC starts by reformulating Eq. (2) into its non-diagonal form

$$G_{+}(\omega) = T_{+}(\omega 1 - M_{+})^{-1} T_{+}^{\dagger},$$
 (3)

where \mathbf{M}_{\pm} is the non-diagonal effective Hamiltonian matrix and \mathbf{T}_{\pm} is the matrix of effective transition moments. The \mathbf{M}_{\pm} and \mathbf{T}_{\pm} matrices are expanded in a perturbative series, which is truncated at order n.

$$\mathbf{M}_{\pm} \approx \mathbf{M}_{\pm}^{(0)} + \mathbf{M}_{\pm}^{(1)} + \dots + \mathbf{M}_{\pm}^{(n)},$$
 (4)

$$T_{+} \approx T_{+}^{(0)} + T_{+}^{(1)} + \dots + T_{+}^{(n)},$$
 (5)

defining the ADC(n) approximation for the propagator.⁵⁸ Diagonalizing the M_{\pm} matrix,

$$\mathbf{M}_{\pm}\mathbf{Y}_{\pm}=\mathbf{Y}_{\pm}\mathbf{\Omega}_{\pm},\tag{6}$$

yields the approximate EAs or IPs, as well as the eigenvectors \mathbf{Y}_{\pm} that can be used to compute the approximate spectroscopic amplitudes $\mathbf{X}_{\pm} = \mathbf{T}_{\pm}\mathbf{Y}_{\pm}$.

B. ADC equations from effective Liouvillian theory

Working equations for the matrix elements of M_\pm and T_\pm can be derived from the algebraic analysis of 1-GF 52 using the intermediate state representation approach 53,58,62,77 or the formalism of effective Liouvillian theory. $^{63,67,78-80}$ Here, we review the equations of single-reference ADC theory derived using the effective Liouvillian approach where the ground-state wavefunction $|\Psi_0^N\rangle$ is assumed to be well-approximated by a reference Slater determinant $|\Phi\rangle$. Generalization of the effective Liouvillian and ADC theories to multiconfigurational reference states has been described elsewhere. $^{49-51,80,81}$

In the single-reference ADC theory, the perturbative expansion in Eqs. (4) and (5) is generated by separating the Hamiltonian H into a zeroth-order contribution

$$H^{(0)} = E_0 + \sum_p \varepsilon_p \{ a_p^{\dagger} a_p \} \tag{7}$$

and a perturbation

$$V = \frac{1}{4} \sum_{pqrs} v_{rs}^{pq} \{ a_p^{\dagger} a_q^{\dagger} a_s a_r \}, \tag{8}$$

where $E_0 = \langle \Phi | H | \Phi \rangle$ is the Hartree–Fock energy, ε_p are the eigenvalues of the canonical Fock matrix (so-called orbital energies)

$$f_p^q = h_q^p + \sum_{i}^{occ} v_{qi}^{pi}, \tag{9}$$

and $h_q^p = \langle p|h|q\rangle$ and $v_{rs}^{pq} = \langle pq \| rs \rangle$ are the one-electron and antisymmetrized two-electron integrals, respectively. Notation $\{\cdots\}$ indicates that the creation and annihilation operators are normal-ordered with respect to the reference determinant $|\Phi\rangle$. Indices p,q,r,s run over all spin-orbitals in a finite one-electron basis set, while i,j,k,l and a,b,c,d index the occupied and virtual orbitals, respectively. We note that the ADC zeroth-order Hamiltonian is equivalent to the one used in single-reference Møller–Plesset perturbation theory. 82

Starting with the zeroth-order Hamiltonian in Eq. (7) and using the effective Liouvillian approach for deriving the ADC equations, we arrive at the expressions for the nth-order contributions to the M_{\pm} and T_{\pm} matrix elements,

$$M_{+\mu\nu}^{(n)} = \sum_{klm}^{k+l+m=n} \langle \Phi | [h_{+\mu}^{(k)}, [\tilde{H}^{(l)}, h_{+\nu}^{(m)\dagger}]]_{+} | \Phi \rangle, \tag{10}$$

$$M_{-\mu\nu}^{(n)} = \sum_{klm}^{k+l+m=n} \langle \Phi | [h_{-\mu}^{(k)\dagger}, [\tilde{H}^{(l)}, h_{-\nu}^{(m)}]]_{+} | \Phi \rangle, \tag{11}$$

$$T_{+pv}^{(n)} = \sum_{kl}^{k+l=n} \langle \Phi | [\tilde{a}_p^{(k)}, h_{+v}^{(l)\dagger}]_+ | \Phi \rangle, \tag{12}$$

$$T_{-p\nu}^{(n)} = \sum_{l=1}^{k+l=n} \langle \Phi | [\tilde{a}_p^{(k)}, h_{-\nu}^{(l)}]_+ | \Phi \rangle. \tag{13}$$

Here, square brackets denote commutators ([A,B]=AB-BA) or anticommutators ($[A,B]_+=AB+BA$). The excitation operators $h_{\pm\mu}^{(m)\dagger}$ are used to form a set of basis states $|\Psi_{\pm\mu}^{(m)}\rangle=h_{\pm\mu}^{(m)\dagger}|\Phi\rangle$ to represent the eigenstates of an $(N\pm1)$ -electron system. For the low-order ADC approximations [up to ADC(3)], only the zeroth-order ($h_{+\mu}^{(0)\dagger}=a_a^\dagger$ and $h_{-\mu}^{(0)\dagger}=a_i$) and first-order ($h_{+\mu}^{(1)\dagger}=a_b^\dagger a_a^\dagger a_i$ and

 $h_{-\mu}^{(1)\dagger}=a_a^\dagger a_j\,a_i$) excitation operators appear in the ADC equations. The $\tilde{H}^{(l)}$ and $\tilde{a}_p^{(l)}$ operators are lth-order contributions to the effective Hamiltonian $\tilde{H}=e^{-(T-T^\dagger)}He^{(T-T^\dagger)}$ and effective observable $\tilde{a}_p=e^{-(T-T^\dagger)}a_pe^{(T-T^\dagger)}$ operators, respectively.

For each block of \mathbf{M}_{\pm} and \mathbf{T}_{\pm} defined by a pair of excitation operators $h_{\pm\mu}^{(m)\dagger}$, the effective operators \tilde{H} and \tilde{a}_p are expanded to different orders. Figure 1 shows the perturbative structure of these matrices for the ADC approximations employed in this work [ADC(2), ADC(2)-X, and ADC(3)]. Explicit expressions for $\tilde{H}^{(l)}$ and $\tilde{a}_p^{(l)}$ are obtained from the Baker–Campbell–Hausdorff (BCH) expansions of \tilde{H} and \tilde{a}_p , e.g.,

$$\tilde{H} = H^{(0)} + V + [H^{(0)}, T^{(1)} - T^{(1)\dagger}] + [H^{(0)}, T^{(2)} - T^{(2)\dagger}]$$

$$+ \frac{1}{2!} [V + (V + [H^{(0)}, T^{(1)} - T^{(1)\dagger}]), T^{(1)} - T^{(1)\dagger}] + \cdots.$$
(14)

These equations depend on the amplitudes of excitation operators $T^{(k)}$,

$$T^{(k)} = \sum_{m}^{N} T_{m}^{(k)},$$

$$T_{m}^{(k)} = \frac{1}{(m!)^{2}} \sum_{iiab...} t_{ij...}^{ab...(k)} a_{a}^{\dagger} a_{b}^{\dagger} \dots a_{j} a_{i},$$
(15)

which are calculated by solving a system of projected amplitude equations. ⁶³ The low-order ADC approximations [ADC(n), $n \le 3$] require calculating up to the nth-order single-excitation amplitudes $(t_i^{a(n)})$ and up to the (n-1)th-order double-excitation amplitudes $(t_{ij}^{abc(n-1)})$. Additionally, the third-order contributions to the T_\pm matrix of ADC(3) formally depend on the triple-excitation amplitudes $(t_{ijk}^{abc(k)})$. ^{77,83} In practice, the $t_{ijk}^{abc(k)}$ contributions are very small and we neglect them in our implementation of ADC(3).

C. Quantifying the spin contamination in ADC calculations

The focus of this work is to investigate the spin contamination in single-reference ADC calculations of charged excited

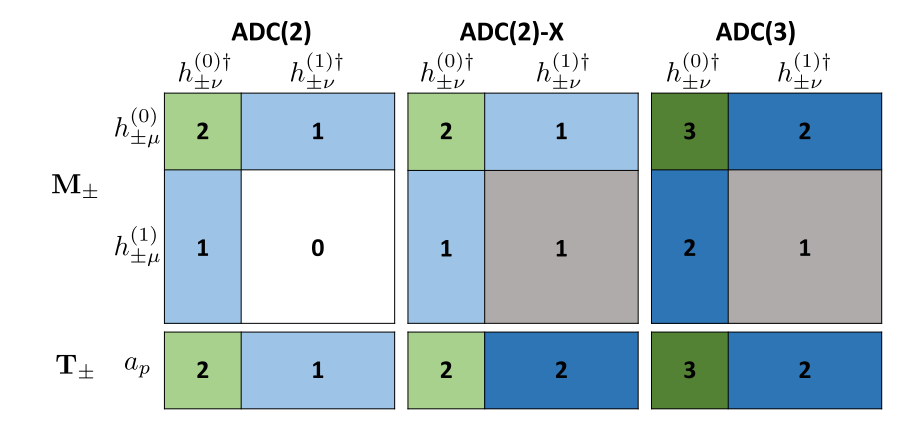


FIG. 1. Perturbative structure of the \mathbf{M}_{\pm} and \mathbf{T}_{\pm} matrices in ADC for charged excitations. Numbers indicate the perturbation order to which the effective Hamiltonian \tilde{H} and observable \tilde{a}_p operators are expanded for a particular block of \mathbf{M}_{\pm} and \mathbf{T}_{\pm} , respectively.

states (EA/IP-ADC) for open-shell molecules. The accuracy of ADC approximations strongly depends on the quality of underlying Hartree–Fock reference wavefunction. In particular, for open-shell molecules, molecular orbitals and orbital energies appearing in the

zeroth-order ADC Hamiltonian in Eq. (7) are usually computed using the unrestricted Hartree–Fock theory (UHF), which may introduce spin contamination into the ADC excited-state energies and properties. Spin contamination can be calculated by subtracting

TABLE I. Open-shell molecules studied in this work and their ground-state spin contamination (a.u.) computed using UHF, MP(n) (n = 2, 3) with the UHF reference, orbital-optimized MP(n) [OMP(n)], and MP(n) with the ROHF reference.

System	State	UHF	MP(2) UHF	MP(3) UHF	OMP(2)	OMP(3)	MP(2) ROHF	MP(3) ROHF
ВеН	$^2\Sigma^+$	0.00	0.00	0.00	0.00	0.00	0.00	0.00
OH	$^{2}\Pi$	0.01	0.00	0.00	0.00	0.00	0.00	0.01
NH_2	2B_1	0.01	0.00	0.00	0.00	0.00	0.00	0.01
SH	$^{2}\Pi$	0.01	0.00	0.00	0.00	0.00	0.01	0.01
CH_3	$^{2}A_{1}^{\prime\prime}$	0.01	0.00	0.00	0.00	0.00	0.00	0.01
SF	$^2\Pi$	0.01	0.00	0.00	0.00	0.00	0.01	0.01
OOH	$^2A^{\prime\prime}$	0.01	0.00	0.00	0.00	0.00	0.01	0.01
CH_2	$^{3}B_{1}$	0.02	0.00	0.00	0.00	0.00	0.01	0.01
NH	$^3\Sigma^-$	0.02	0.00	0.00	0.00	0.00	0.01	0.01
PH_2	$^{2}B_{1}$	0.02	0.00	0.00	0.00	0.00	0.01	0.01
Si ₂	$^3\Sigma^-$	0.02	0.00	0.00	0.00	0.00	0.01	0.01
SiF	$^2\Pi$	0.02	0.00	0.01	0.00	0.00	0.01	0.01
FO	$^2\Pi$	0.04	0.02	0.02	0.00	0.00	0.00	0.01
O_2	$3\sum_{g}^{-}$ $3\sum_{g}^{-}$ $2\sum_{g}^{+}$	0.05	0.01	0.02	0.00	0.00	0.02	0.02
S_2	$^{3}\Sigma_{\sigma}^{\frac{s}{c}}$	0.05	0.01	0.02	0.00	0.00	0.02	0.02
ВО	$^{2}\Sigma^{+}$	0.06	0.03	0.04	0.00	0.01	0.00	0.01
BN	$^{3}\Pi$	0.06	0.04	0.04	0.00	0.00	0.00	0.01
SO	$^3\Sigma^-$	0.06	0.02	0.02	0.00	0.00	0.02	0.02
NO	$^2\Pi$	0.10	0.07	0.07	0.00	0.00	0.01	0.01
NCO	$^2\Pi$	0.11	0.06	0.06	0.00	0.01	0.01	0.01
AlO	$^2\Sigma^+$	0.13	0.09	0.10	0.00	0.00	0.01	0.01
CNC	$^{2}\Pi_{g}$	0.14	0.07	0.08	0.00	0.00	0.02	0.03
NO_2	${}^{2}A_{1}^{3}$	0.14	0.10	0.11	0.00	0.00	0.01	0.01
CH ₂ CHO	$^{2}A^{\prime\prime}$	0.19	0.11	0.12	0.00	0.01	0.01	0.01
C_4O	$^3\Sigma^-$	0.21	0.12	0.13	0.02	0.02	0.03	0.02
BP	$^{3}\Pi$	0.22	0.17	0.18	0.00	0.00	0.01	0.01
C_3H_5	$^{2}A_{2}$	0.22	0.13	0.13	-0.01	0.01	0.03	0.04
N ₃	$^{2}\Pi_{\sigma}$	0.23	0.14	0.15	0.01	0.01	0.03	0.02
SCN	$^{2}\Pi_{g}$ $^{2}\Pi$	0.24	0.14	0.15	0.00	0.01	0.01	0.01
CH_2CN	$^{2}B_{1}$	0.24	0.14	0.15	0.00	0.01	0.01	0.01
C_2H_3	$^{2}A'$	0.25	0.17	0.18	0.00	0.01	0.00	0.01
CNN	$^3\Sigma^-$	0.26	0.14	0.14	0.00	0.01	0.03	0.04
C_3H_3	$^{2}B_{1}$	0.27	0.16	0.17	0.00	0.01	0.01	0.02
CH	$^2\Pi$	0.33	0.33	0.33	0.00	0.00	0.01	0.01
CHN ₂	$^2A^{\prime\prime}$	0.36	0.24	0.25	0.00	0.01	0.02	0.02
HCCN	$^3A''$	0.40	0.23	0.24	-0.01	0.02	0.02	0.03
CN	$^2\Sigma^+$	0.49	0.36	0.36	0.00	0.01	0.01	0.01
NS	$^{2}\Pi$	0.51	0.41	0.42	0.00	0.01	0.01	0.01
SiC	$^{3}\Pi$	0.58	0.49	0.49	0.00	0.02	0.01	0.02
CP	$^{2}\Sigma^{+}$	0.97	0.79	0.79	0.00	0.05	0.01	0.01
Average		0.18	0.12	0.12	0.00	0.01	0.01	0.01
Sum		7.03	4.84	4.98	0.02	0.25	0.45	0.54

the computed expectation value of the spin-squared operator (S^2) from its exact eigenvalue for a particular electronic state, ^{84–86}

$$\Delta S^2 \equiv \langle S^2 \rangle_{computed} - \langle S^2 \rangle_{exact}. \tag{16}$$

Here, we present an approach based on effective Liouvillian theory that allows us to compute the S^2 expectation values and spin contamination in the ADC calculations. To the best of our knowledge, this work is the first study of excited-state spin contamination in ADC. An investigation of spin contamination in the related CC2 method has been reported recently.⁸⁷

A general expression for the expectation value of spin-squared operator with respect to a wavefunction $|\Psi\rangle$ has the form $^{88-91}$

$$\langle S^2 \rangle = \frac{1}{4} \left(\sum_{p \in \alpha} \gamma_p^p - \sum_{\tilde{p} \in \beta} \gamma_{\tilde{p}}^{\tilde{p}} \right)^2 + \frac{1}{2} \left(\sum_{p \in \alpha} \gamma_p^p + \sum_{\tilde{p} \in \beta} \gamma_{\tilde{p}}^{\tilde{p}} \right) + \sum_{\substack{p,s \in \alpha \\ \tilde{q}, \tilde{r} \in \beta}} S_s^{\tilde{p}} S_s^{\tilde{q}} \Gamma_{\tilde{r}s}^{p\tilde{q}}, \quad (17)$$

where we use a bar to distinguish between the spin-orbitals with α and β spin, γ_q^p and Γ_{rs}^{pq} are the one- and two-particle reduced density matrices

$$\gamma_q^p = \langle \Psi | a_p^{\dagger} a_q | \Psi \rangle, \quad \Gamma_{rs}^{pq} = \langle \Psi | a_p^{\dagger} a_q^{\dagger} a_s a_r | \Psi \rangle,$$
(18)

and $S_{\bar{q}}^{p}$ is the overlap of two spatial molecular orbitals with opposite spin,

$$S_{\bar{a}}^{p} = \langle \phi_{p} | \phi_{q} \rangle, \quad \phi_{p} \in \alpha, \ \phi_{q} \in \beta.$$
 (19)

Evaluating $\langle S^2 \rangle$ for a charged excited state $|\Psi \rangle$ requires calculating the excited-state one- and two-particle reduced density matrices [Eq. (18)], which are the expectation values of one- and two-body operators $(O=a_p^\dagger a_q,\ a_p^\dagger a_q^\dagger a_s a_r)$ with respect to $|\Psi \rangle$. An approach to evaluate the operator expectation values in ADC using intermediate state representation has been presented by Trofimov, Dempwolff, and co-workers. 55,59,64,65,68,92-94 Below, we demonstrate how the ADC excited-state reduced density matrices and the expectation values of spin-squared operator can be computed within the framework of effective Liouvillian theory.

The expectation value of an arbitrary operator O for an excited state described by the ADC eigenvector $Y_{\pm uI}$ has the form

$$\langle O \rangle_{\pm I} = \sum_{(n)}^{(m)} \sum_{\mu\nu} Y_{\pm I\mu}^{\dagger} O_{\pm \mu\nu}^{(n)} Y_{\pm \nu I}, \tag{20}$$

where $O_{\pm\mu\nu}^{(n)}$ is the *n*th-order matrix element of the operator O and the summation over (n) includes all contributions up to the order of ADC approximation (m). In order to obtain the expressions for $O_{\pm\mu\nu}^{(n)}$, we separate these matrix elements into a reference (ground-state) contribution $O_0^{(n)}$ and the excitation component $\Delta O_{\pm\mu\nu}^{(n)}$,

$$O_{\pm\mu\nu}^{(n)} = O_0^{(n)} \delta_{\mu\nu} \pm \Delta O_{\pm\mu\nu}^{(n)}.$$
 (21)

Equations for $\Delta O_{\pm\mu\nu}^{(n)}$ can be obtained by analogy with Eqs. (10) and (11) for the matrix elements of the shifted effective Hamiltonian.

TABLE II. Vertical electron affinities (eV) of weakly spin-contaminated open-shell molecules computed using EA-ADC, EA-EOM-CCSD, and CCSD(T) with various reference wavefunctions (UHF, OMP, and ROHF). The aug-cc-pVDZ basis set was used in all calculations. Also shown are mean absolute errors (MAEs) and standard deviations (STDVs) relative to the CCSD(T) results.

System	Transition	ADC(2) UHF	ADC(2)-X UHF	ADC(3) UHF	ADC(2) OMP(2)	ADC(2)-X OMP(2)	ADC(3) OMP(3)	ADC(2) ROHF	ADC(2)-X ROHF	ADC(3) ROHF	EOM-CCSD UHF	CCSD(T) ROHF
ВеН	$^2\Sigma^+ \rightarrow ^1\Sigma^+$	-0.01	0.53	0.47	0.00	0.54	0.48	0.00	0.54	0.48	0.42	0.48
OH	$^{2}\Pi \rightarrow {}^{1}\Sigma^{+}$	1.33	2.11	1.22	1.80	2.60	1.21	1.41	2.22	1.27	1.50	1.63
NH_2	$^2B_1 \rightarrow {}^1A_1$	0.35	0.95	0.16	0.64	1.26	0.22	0.44	1.07	0.22	0.41	0.54
SH	$^{2}\Pi \rightarrow {}^{1}\Sigma^{+}$	1.99	2.47	2.01	2.10	2.60	2.04	2.05	2.55	2.05	2.05	2.12
CH_3	$^2A_1^{\prime\prime} \rightarrow \ ^1A_1^{\prime}$	-0.49	0.03	-0.47	-0.37	0.18	-0.39	-0.40	0.15	-0.40	-0.36	-0.24
SF	$^{2}\Pi \rightarrow {}^{1}\Sigma^{+}$	1.98	2.45	2.00	2.04	2.51	2.08	2.05	2.53	2.04	2.02	2.08
OOH	$^2A^{\prime\prime} \rightarrow {}^1A^{\prime}$	0.41	1.00	0.31	0.68	1.31	0.31	0.56	1.17	0.38	0.24	0.47
CH_2	$^3B_1 \rightarrow ^2B_1$	-0.42	0.23	-0.19	-0.30	0.38	-0.11	-0.36	0.32	-0.14	-0.11	0.02
NH	$^3\Sigma^- \rightarrow {}^2\Pi$	-0.36	0.37	-0.18	-0.14	0.63	-0.10	-0.27	0.50	-0.11	-0.06	0.06
PH_2	$^2B_1 \rightarrow {}^1A_1$	0.89	1.32	0.95	0.98	1.41	1.00	0.97	1.42	1.01	0.97	1.04
Si_2	$^3\Sigma^- \rightarrow {}^2\Pi_u$	2.01	2.35	1.85	2.06	2.39	1.84	2.04	2.38	1.87	1.85	1.94
SiF	$^{2}\Pi \rightarrow ^{3}\Sigma^{-}$	0.70	1.02	0.84	0.69	1.02	0.86	0.74	1.07	0.87	0.71	0.78
FO	$^{2}\Pi \rightarrow {}^{1}\Sigma_{g}^{+}$	1.91	2.46	1.47	2.06	2.69	1.62	2.10	2.62	1.50	1.66	1.83
O_2	$^{3}\Sigma_{g}^{-} \rightarrow ^{2}\Pi_{g}$	-0.73	-0.15	-0.41	-0.43	0.23	-0.28	-0.51	0.12	-0.09	-0.53	-0.28
S_2	${}^{3}\Sigma_{g}^{-} \rightarrow {}^{2}\Pi_{g}$ ${}^{2}\Sigma^{+} \rightarrow {}^{1}\Sigma^{-}$	1.31	1.62	1.33	1.42	1.73	1.34	1.31	1.64	1.40	1.27	1.33
BO		2.15	2.65	2.10	2.09	2.59	2.30	2.26	2.76	2.18	2.29	2.36
BN	$^{3}\Pi \rightarrow ^{2}\Sigma^{+}$	2.92	3.42	2.46	3.36	3.79	2.40	2.92	3.43	2.49	2.71	2.91
SO	$^3\Sigma^- \rightarrow {}^2\Pi$	0.62	1.01	0.84	0.81	1.22	0.84	0.63	1.05	1.00	0.69	0.83
MAE	·	0.20	0.33	0.18	0.17	0.51	0.14	0.16	0.42	0.16	0.12	
STDV		0.18	0.15	0.15	0.22	0.25	0.16	0.18	0.17	0.18	0.06	

Simplifying Eqs. (10) and (11) and replacing H by O, we obtain

$$\Delta O_{+\mu\nu}^{(n)} = \sum_{klm}^{k+l+m=n} \left(\langle \Phi | h_{+\mu}^{(k)} \tilde{O}^{(l)} h_{+\nu}^{(m)\dagger} | \Phi \rangle - \delta_{\mu\nu} \delta_{km} \langle \Phi | \tilde{O}^{(l)} | \Phi \rangle \right), \quad (22)$$

$$\Delta O_{-\mu\nu}^{(n)} = \sum_{klm}^{k+l+m=n} \left(-\langle \Phi | h_{-\nu}^{(m)} \tilde{O}^{(l)} h_{-\mu}^{(k)\dagger} | \Phi \rangle + \delta_{\mu\nu} \delta_{km} \langle \Phi | \tilde{O}^{(l)} | \Phi \rangle \right), \tag{23}$$

where $\tilde{O}^{(l)}$ is the *l*th-order contribution to an effective operator $\tilde{O} = e^{-(T-T^{\dagger})} O e^{(T-T^{\dagger})}$ that can be obtained from its BCH expansion,

$$\tilde{O} = O^{(0)} + [O^{(0)}, T^{(1)} - T^{(1)\dagger}] + [O^{(0)}, T^{(2)} - T^{(2)\dagger}]
+ \frac{1}{2!} [[O^{(0)}, T^{(1)} - T^{(1)\dagger}], T^{(1)} - T^{(1)\dagger}] + \cdots .$$
(24)

Identifying the second term on the rhs of Eqs. (22) and (23) as $O_0^{(n)} \delta_{\mu\nu}$, moving it to the lhs, and inverting the sign of Eq. (23), we obtain the expressions for $O_{\pm\mu\nu}^{(k)}$ of an arbitrary operator,

$$O_{+\mu\nu}^{(n)} = \sum_{l=1,\dots}^{k+l+m=n} \langle \Phi | h_{+\mu}^{(k)} \tilde{O}^{(l)} h_{+\nu}^{(m)\dagger} | \Phi \rangle, \tag{25}$$

$$O_{-\mu\nu}^{(n)} = \sum_{\substack{k+lm=n\\ \mu}}^{k+l+m=n} \langle \Phi | h_{-\nu}^{(m)} \tilde{O}^{(l)} h_{-\mu}^{(k)\dagger} | \Phi \rangle.$$
 (26)

Combining Eq. (20) with Eqs. (25) and (26) for $O = a_p^{\dagger} a_q$ and $a_p^{\dagger} a_q^{\dagger} a_s a_r$, we obtain the working equations for one- and two-particle reduced density matrices of charged excited states for an arbitrary-order ADC approximation. As an example, we present the equations for y_q^p and Γ_{rs}^{pq} of ADC(2) in the supplementary material. Once the excited-state y_q^p and Γ_{rs}^{pq} are computed, we evaluate the corresponding expectation values of spin-squared operator and spin contamination according to Eqs. (16) and (17).

D. Reducing the spin contamination in ADC using the ROHF and OMP(n) reference orbitals

To reduce the spin contamination in ADC calculations of charged excitations for open-shell molecules, we combined our EA/IP-ADC implementation with the reference orbitals from (i) restricted open-shell Hartree–Fock (ROHF)⁶⁹ and (ii) orbital-optimized nth-order Møller–Plesset perturbation [OMP(n)] theories. $^{30-33,70-73}$ These reference wavefunctions are known to either completely eradicate or significantly reduce the spin

TABLE III. Vertical electron affinities (eV) of strongly spin-contaminated open-shell molecules computed using EA-ADC, EA-EOM-CCSD, and CCSD(T) with various reference wavefunctions (UHF, OMP, and ROHF). The aug-cc-pVDZ basis set was used in all calculations. Also shown are mean absolute errors (MAEs) and standard deviations (STDVs) relative to the CCSD(T) results.

System	Transition	ADC(2) UHF	ADC(2)-X UHF	ADC(3) UHF	ADC(2) OMP(2)	ADC(2)-X OMP(2)	ADC(3) OMP(3)		ADC(2)-X ROHF	ADC(3) ROHF	EOM-CCSD UHF	CCSD(T) ROHF
NO	$^2\Pi \rightarrow ^3\Sigma^-$	-0.59	-0.04	-0.27	-0.62	-0.07	-0.28	-0.60	-0.08	-0.41	-0.66	-0.49
NCO	$^{2}\Pi \rightarrow ^{1}\Sigma^{+}$	3.41	3.74	2.95	3.87	3.78	3.03	3.82	4.13	3.05	3.14	3.28
AlO	$^2\Sigma^+ \rightarrow ^1\Sigma^+$	2.60	3.46	2.63	3.26	4.15	2.60	2.24	2.65	2.84	2.84	2.51
CNC	$^{2}\Pi_{g} \rightarrow ^{3}\Sigma_{g}^{-}$	2.09	2.42	1.90	2.26	2.51	1.86	2.25	2.47	1.82	1.84	1.87
NO_2	$^2A_1 \rightarrow {}^1A_1$	1.35	1.70	1.22	1.33	1.76	1.44	1.41	1.78	1.27	1.21	1.33
CH_2CHO	$^2A^{\prime\prime} \rightarrow {}^1A^{\prime}$	1.26	1.69	1.16	1.77	2.14	1.28	1.63	2.00	1.31	1.24	1.49
C_4O	$^3\Sigma^- \rightarrow {}^2\Pi$	2.97	3.20	2.47	3.19	3.26	2.56	3.22	3.37	2.57	2.60	2.68
BP	$^{3}\Pi \rightarrow {}^{4}\Sigma^{-}$	2.55	2.94	2.37	2.72	3.05	2.36	2.63	2.99	2.39	2.42	2.53
C_3H_5	$^2A_2 \rightarrow ^1A_1$	-0.03	0.34	-0.18	0.52	0.86	0.05	0.43	0.76	0.12	-0.04	0.20
N_3	$^{2}\Pi_{g} \rightarrow ^{1}\Sigma_{g}^{+}$	2.85	3.05	2.01	3.44	3.45	2.14	3.14	3.23	2.31	2.34	2.52
SCN	$^{2}\Pi \rightarrow ^{1}\Sigma^{+}$	3.33	3.66	3.13	3.71	3.99	3.27	3.61	3.93	3.29	3.24	3.35
CH_2CN	$^2B_1 \rightarrow {}^1A_1$	1.22	1.58	0.98	1.60	1.93	1.17	1.59	1.93	1.16	1.16	1.33
C_2H_3	$^2A' \rightarrow ^1A'$	-0.22	0.28	-0.28	0.18	0.64	-0.14	0.15	0.61	-0.15	-0.14	0.07
CNN	$^3\Sigma^- \rightarrow {}^2\Pi$	1.41	1.86	1.17	2.15	2.42	1.31	1.73	2.14	1.49	1.31	1.51
C_3H_3	$^2B_1 \rightarrow {}^1A_1$	0.35	0.70	0.16	0.80	1.12	0.37	0.76	1.10	0.41	0.32	0.52
CH	$^{2}\Pi \rightarrow {}^{3}\Sigma^{-}$	0.72	1.43	1.04	1.01	1.64	1.14	0.95	1.57	1.13	0.97	1.08
CHN_2	$^2A^{\prime\prime} \rightarrow {}^1A^{\prime}$	1.62	1.92	1.08	2.16	2.24	1.18	1.97	2.19	1.34	1.30	1.49
HCCN	$^3A^{\prime\prime} \rightarrow {}^2A^{\prime\prime}$	1.11	1.59	1.10	1.71	2.10	1.32	1.63	2.07	1.30	1.24	1.46
CN	$^2\Sigma^+ \rightarrow ^1\Sigma^+$	3.49	4.08	3.49	3.60	4.10	3.76	4.25	4.62	3.59	3.52	3.69
NS	$^{2}\Pi \rightarrow {}^{3}\Sigma^{-}$	1.32	1.73	1.44	1.06	1.34	1.14	1.24	1.52	1.03	0.94	0.95
SiC	$^{3}\Pi \rightarrow ^{2}\Sigma^{+}$	2.05	2.49	1.97	2.70	2.96	1.93	2.34	2.72	1.94	2.03	2.19
CP	$^{2}\Sigma^{+} \rightarrow ^{1}\Sigma^{+}$	2.23	2.88	2.08	3.43	3.54	2.28	3.69	3.78	2.17	2.39	2.70
MAE		0.20	0.38	0.29	0.37	0.66	0.18	0.31	0.60	0.15	0.17	
STDV		0.23	0.20	0.25	0.29	0.26	0.17	0.28	0.19	0.16	0.13	

contamination in state-specific (usually, ground-state) calculations of open-shell systems. ^{30,72,87,95–97}

To combine EA/IP-ADC with ROHF, we use the approach developed by Knowles and co-workers⁹⁵ in restricted open-shell Møller-Plesset perturbation theory. Following this approach, the ROHF-based ADC methods [ADC(n)/ROHF] can be implemented by modifying the unrestricted ADC implementation [ADC(n)/UHF] as described below.

Using the ROHF orbitals, we calculate the Fock matrices [Eq. (9)] for spin-up (α) and spin-down (β) electrons and semicanonicalize them following the procedure described in Ref. 95. The diagonal Fock matrix elements calculated in the semicanonical basis are used to define the ADC zeroth-order Hamiltonian in Eq. (7). The off-diagonal Fock matrix elements (fⁱ_a) are included in the perturbation operator V, which now has the form

$$V = \frac{1}{4} \sum_{pqrs} v_{rs}^{pq} \left\{ a_p^{\dagger} a_q^{\dagger} a_s a_r \right\} + \sum_{ia} \left(f_a^i \left\{ a_i^{\dagger} a_a \right\} + f_i^a \left\{ a_a^{\dagger} a_i \right\} \right). \tag{27}$$

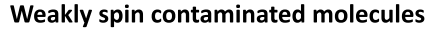
2. The f_a^i terms in V significantly modify the ADC equations. First, these contributions give rise to the f_a^i -dependent terms

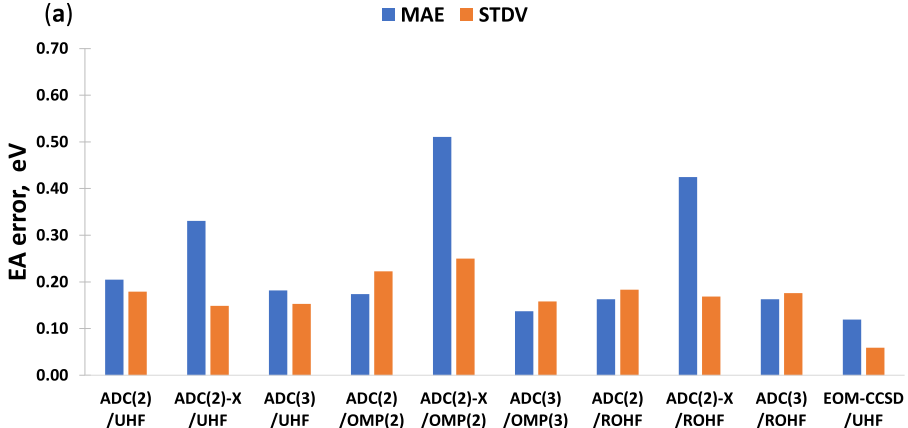
in effective Hamiltonian matrix \mathbf{M}_{\pm} . Second, for V in Eq. (27), the Brillouin theorem is no longer satisfied and the first-order single-excitation amplitudes in excitation operator $T^{(1)}$ [Eq. (15)] have nonzero values,

$$t_i^{a(1)} = \frac{f_i^a}{\varepsilon_i - \varepsilon_a}. (28)$$

The $t_i^{a(1)}$ terms enter the projected amplitude equations for other amplitudes and give rise to new contributions in the equations for all ADC matrices.

An alternative approach to mitigate spin contamination that we explore in this work is to combine the ADC(n) methods with orbitals from the OMP(n) calculations [ADC(n)/OMP(n)]. Orbital optimization has been shown to significantly reduce spin contamination and improve the accuracy of correlated (post-Hartree–Fock) calculations for open-shell molecules. ^{26–37} Considering the close relationship between ADC and Møller–Plesset perturbation theories, using the OMP(n) orbitals to perform the ADC(n) calculations is a promising alternative to the UHF reference orbitals for molecules with unpaired electrons.





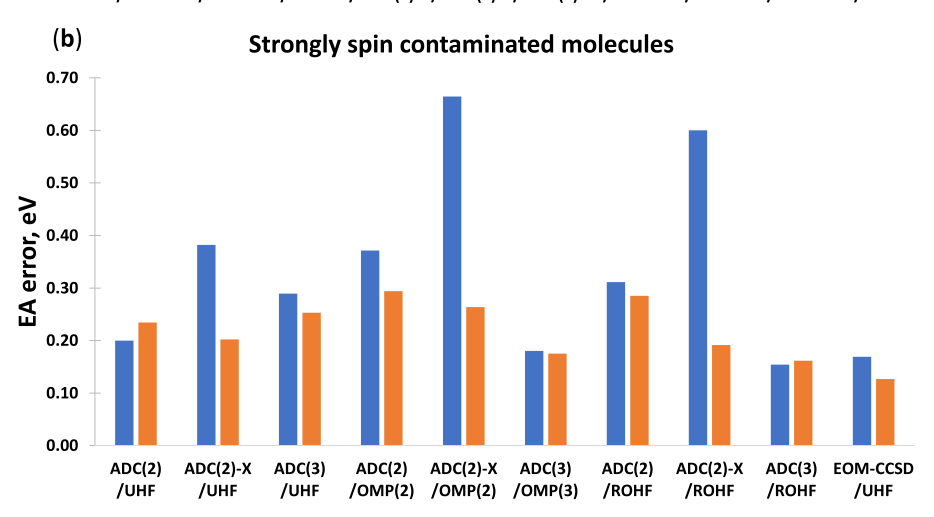


FIG. 2. Mean absolute errors (MAEs) and standard deviations (STDVs) in the EA-ADC vertical electron affinities (eV) for (a) 18 weakly and (b) 22 strongly spin-contaminated molecules with the ground-state UHF spin contamination of <0.1 and ≥0.1 a.u., respectively. Reference data are from CCSD(T). The aug-cc-pVDZ basis set was used. See Tables II and III for data on individual molecules.

We refer the readers interested in details of orbital-optimized Møller–Plesset perturbation theory to excellent publications on this subject. $^{30-32}$ As for the ROHF reference, combining ADC(n) with the OMP(n) orbitals requires several modifications to the UHF-based ADC methods as outlined below:

- 1. Upon successful completion of the reference OMP(n) calculation, the Fock matrices for α and β -electrons are semicanonicalized as described for ADC(n)/ROHF. The diagonal Fock matrix elements are used to define the ADC zeroth-order Hamiltonian in Eq. (7), while the off-diagonal f_a^i elements enter the expression for the perturbation operator in Eq. (27).
- 2. The f_a^i contributions in Eq. (27) give rise to new terms in the effective Hamiltonian matrix \mathbf{M}_{\pm} .
- 3. As in the reference OMP(n) calculations, all single-excitation amplitudes and the corresponding projections of the effective Hamiltonian are assumed to be zero in all ADC equations $(t_i^{a(k)} \approx 0 \text{ and } \langle \Phi | a_i^{\dagger} a_a \tilde{H}^{(k)} | \Phi \rangle \approx 0, \forall k)$.
- 4. The converged OMP(n) double-excitation amplitudes $(t_{ij}^{ab(k)})$ are transformed to the semicanonical basis³⁵ and are used to compute the ADC matrix elements.

Working equations for the ROHF-based EA/IP-ADC(n) methods are provided in the supplementary material. The equations for EA/IP-ADC(n) combined with the OMP(n) reference orbitals can be obtained by setting the terms depending on single-excitation amplitudes to zero.

III. COMPUTATIONAL DETAILS

The ROHF- and OMP(n)-based EA/IP-ADC(2), EA/IP-ADC(2)-X, and EA/IP-ADC(3) methods were implemented in the developer's version of PySCF98 by modifying the existing unrestricted ADC module. Additionally, for each reference [UHF, ROHF, and OMP(n)], we implemented the subroutines for calculating one- and two-particle reduced density matrices [Eq. (18)], the expectation values of spin-squared operator [Eq. (17)], and spin contamination [Eq. (16)]. Our implementation of the ADC reduced density matrices was validated by reproducing the EA/IP-ADC(2)/UHF dipole moments of charged states reported by Dempwolff and co-workers.^{64,68} For EA/IP-ADC(3), the reduced density matrices incorporated contributions up to the third order in perturbation theory. We are aware of only one previous implementation of EA/IP-ADC(n) with the ROHF reference in the Q-Chem package. 99 Numerical tests of both EA/IP-ADC(n)/ROHFprograms (PySCF and Q-Chem) indicate that they produce very similar results when the contributions from first-order single excitations [Eq. (28)] are neglected in our PySCF implementation, suggesting that these excitations may be missing in the Q-Chem implementation of ADC(n)/ROHF. To the best of our knowledge, our work represents the first implementation of the EA/IP-ADC(n)/OMP(n) methods. Specifically, the EA/IP-ADC(2)and EA/IP-ADC(2)-X methods were combined with the OMP(2) reference orbitals, while for EA/IP-ADC(3), we used the OMP(3) reference.

TABLE IV. Vertical ionization energies (eV) of weakly spin-contaminated open-shell molecules computed using IP-ADC, IP-EOM-CCSD, and CCSD(T) with various reference wavefunctions (UHF, OMP, and ROHF). The aug-cc-pVDZ basis set was used in all calculations. Also shown are mean absolute errors (MAEs) and standard deviations (STDVs) relative to the CCSD(T) results.

System	Transition	ADC(2) UHF	ADC(2)-X UHF	ADC(3) UHF	ADC(2) OMP(2)	ADC(2)-X OMP(2)	ADC(3) OMP(3)	ADC(2) ROHF	ADC(2)-X ROHF	ADC(3) ROHF	EOM-CCSD UHF	CCSD(T) ROHF
ВеН	$^2\Sigma^+ \rightarrow ^1\Sigma^+$	8.34	8.18	8.28	8.31	8.15	8.25	8.34	8.18	8.28	8.32	8.31
OH	$^{2}\Pi \rightarrow {}^{3}\Sigma^{-}$	11.79	11.91	13.03	11.99	12.16	12.91	11.76	11.90	13.05	12.64	12.75
NH_2	$^2B_1 \rightarrow {}^3B_1$	11.15	11.11	11.95	11.24	11.23	11.94	11.14	11.11	11.97	11.78	11.85
SH	$^{2}\Pi \rightarrow {}^{3}\Sigma^{-}$	9.79	9.62	9.99	9.81	9.65	9.99	9.79	9.63	9.99	10.03	10.01
CH_3	$^2A_1^{\prime\prime} \rightarrow \ ^1A_1^{\prime}$	9.40	9.15	9.64	9.34	9.10	9.63	9.34	9.11	9.61	9.60	9.64
SF	$^{2}\Pi \rightarrow ^{3}\Sigma^{-}$	9.79	9.70	10.09	9.75	9.68	10.13	9.79	9.70	10.08	10.19	10.11
OOH	$^2A^{\prime\prime} \rightarrow {}^3A^{\prime\prime}$	10.70	10.55	11.74	10.31	10.23	11.64	10.70	10.55	11.76	11.43	11.40
CH_2	$^3B_1 \rightarrow ^2A_1$	10.11	9.81	10.27	10.08	9.80	10.25	10.07	9.78	10.26	10.24	10.27
NH	$^3\Sigma^- \rightarrow {}^2\Pi$	13.04	12.68	13.41	13.07	12.74	13.38	13.01	12.66	13.39	13.29	13.33
PH_2	$^2B_1 \rightarrow {}^1A_1$	9.64	9.29	9.62	9.58	9.25	9.61	9.59	9.26	9.61	9.67	9.65
Si_2	$^3\Sigma^- \rightarrow ^4\Sigma^-$	7.51	7.20	7.59	7.35	7.07	7.55	7.47	7.18	7.57	7.74	7.66
SiF	$^{2}\Pi \rightarrow ^{1}\Sigma^{+}$	7.42	7.20	7.43	7.32	7.11	7.42	7.36	7.16	7.42	7.52	7.47
FO	$^{2}\Pi \rightarrow ^{3}\Sigma^{-}$	11.88	11.78	12.96	11.71	11.73	13.04	11.89	11.81	12.97	13.49	12.82
O_2	$^{3}\Sigma_{g}^{-} \rightarrow ^{2}\Pi_{g}$	11.26	10.99	12.39	11.01	10.88	12.52	11.30	11.09	12.41	12.09	12.24
S_2	$^{3}\Sigma_{g}^{-} \rightarrow ^{2}\Pi_{g}$	8.95	8.61	9.33	8.77	8.52	9.34	8.91	8.65	9.31	9.28	9.27
ВО	$^{2}\Sigma^{+} \rightarrow ^{1}\Sigma$	12.61	12.81	13.17	12.51	12.50	13.18	12.63	12.76	13.04	13.22	12.95
BN	$^{3}\Pi \rightarrow {}^{4}\Sigma^{-}$	10.49	10.34	11.25	10.71	10.71	11.16	10.57	10.51	11.23	11.25	11.28
SO	$^3\Sigma^- \rightarrow {}^2\Pi$	9.52	9.45	10.39	9.22	9.36	10.44	9.24	9.46	10.38	10.28	10.27
MAE		0.44	0.60	0.09	0.51	0.63	0.11	0.47	0.60	0.10	0.10	
STDV		0.35	0.31	0.12	0.39	0.31	0.13	0.35	0.28	0.13	0.18	

To benchmark the accuracy of EA/IP-ADC(n) with the UHF, ROHF, and OMP(n) references, we performed the calculations of vertical electron affinities (EA), vertical ionization energies (IP), and excited-state spin contamination for the lowestenergy charged states of 40 neutral open-shell molecules shown in Table I. These systems were classified into two groups based on the spin contamination (ΔS^2) in reference UHF calculation: (i) 18 weakly spin-contaminated molecules (WSM) with $\Delta S^2 < 0.1$ a.u. and (ii) 22 strongly spin-contaminated molecules (SSM) with $\Delta S^2 \ge 0.1$ a.u. The equilibrium geometries of all molecules were computed using coupled cluster theory with single, double, and perturbative triple excitations combined with the ROHF reference [CCSD(T)/ROHF]^{19,20,100–102} and are reported in the supplementary material. The vertical EAs and IPs from CCSD(T)/ROHF were used to benchmark the accuracy of EA/IP-ADC(n) with the UHF, ROHF, and OMP(n) references. For comparison, we also report the EAs and IPs from equation-of-motion coupled cluster theory with single and double excitations (EOM-CCSD). 19-25 In all calculations, the aug-cc-pVDZ basis set¹⁰³ was used. All coupled cluster results were obtained using the Q-Chem¹⁰⁴ and CFOUR¹⁰⁵ software packages. Throughout the manuscript, positive electron affinity indicates exothermic electron attachment (i.e., EA = $E_N - E_{N+1}$) while a positive ionization energy corresponds to an endothermic process $(IP = E_{N-1} - E_N).$

IV. RESULTS AND DISCUSSION

A. Benchmarking EA/IP-ADC with the unrestricted (UHF) reference

We begin by analyzing the errors in vertical electron affinities (EAs) computed using EA-ADC/UHF for weakly and strongly spin-contaminated open-shell molecules (WSM and SSM), as defined in Sec. III. The EA-ADC/UHF and EA-EOM-CCSD/UHF electron affinities for both sets of molecules are shown in Tables II and III, along with the reference results from CCSD(T)/ROHF. Figure 2 illustrates how the mean absolute errors (MAEs) and standard deviation of errors (STDV) change with increase in the level of EA-ADC theory. For WSM, MAE reduces in the following order: EA-ADC(2)-X (0.33 eV) > EA-ADC(2) (0.21 eV)> EA-ADC(3) (0.18 eV), in very good agreement with the benchmark results from Ref. 63. This trend changes for SSM where the MAE of EA-ADC(2) remains low (0.20 eV), but EA-ADC(2)-X and EA-ADC(3) show significantly larger errors than for WSM (MAE = 0.38 and 0.29 eV, respectively). Increasing spin contamination in the UHF reference wavefunction also affects STDV for all three methods, which grows by at least 33% for EA-ADC(2) and as much as 80% for EA-ADC(3). The EA-EOM-CCSD/UHF method shows the smallest MAE and STDV out of all UHF-based methods considered in this study for SSM, indicating that it is less

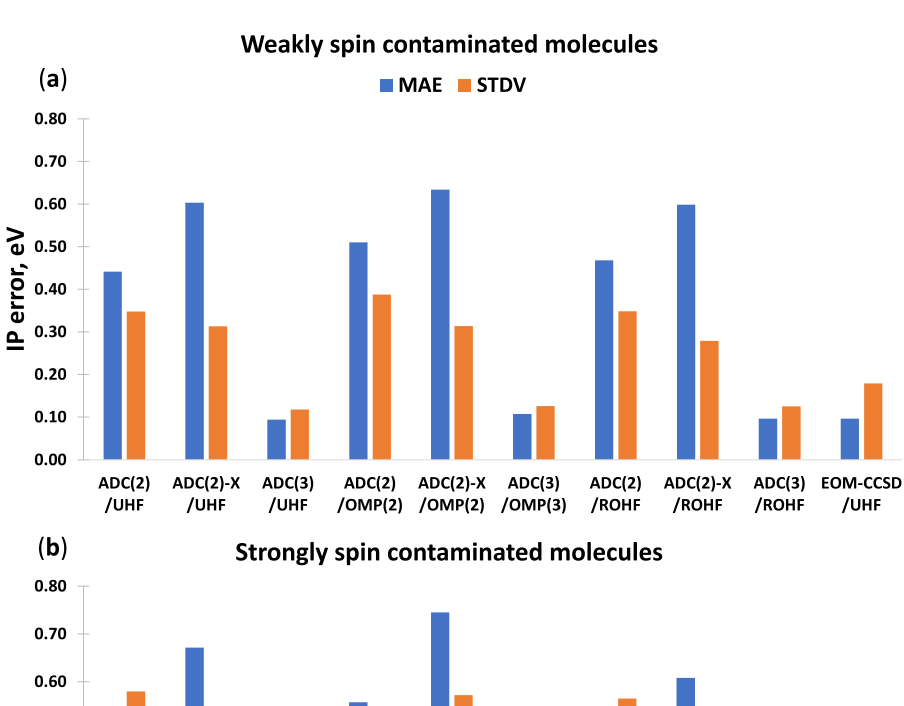
TABLE V. Vertical ionization energies (eV) of strongly spin-contaminated open-shell molecules computed using IP-ADC, IP-EOM-CCSD, and CCSD(T) with various reference wavefunctions (UHF, OMP, and ROHF). The aug-cc-pVDZ basis set was used in all calculations. Also shown are mean absolute errors (MAEs) and standard deviations (STDVs) relative to the CCSD(T) results.

System	Transition	ADC(2) UHF	ADC(2)-X UHF	ADC(3) UHF	ADC(2) OMP(2)	ADC(2)-X OMP(2)	ADC(3) OMP(3)	` '	ADC(2)-X ROHF	ADC(3) ROHF	EOM-CCSD UHF	CCSD(T) ROHF
NO	$^2\Pi \rightarrow ^1\Sigma^+$	8.92	8.83	9.71	8.66	8.68	9.78	8.94	8.85	9.56	9.56	9.54
NCO	$^{2}\Pi \rightarrow {}^{3}\Sigma^{-}$	11.14	11.08	11.57	11.14	11.20	11.70	11.22	11.19	11.61	11.70	11.69
AlO	$^{2}\Sigma^{+} \rightarrow ^{1}\Sigma^{+}$	9.00	8.69	9.05	8.96	8.74	9.20	7.98	8.89	9.89	9.26	9.88
CNC	$^{2}\Pi_{g} \rightarrow {}^{1}\Sigma_{g}^{+}$	9.72	9.34	9.66	9.31	9.03	9.58	9.55	9.27	9.52	9.78	9.54
NO_2	$^2A_1 \rightarrow {}^1A_1$	10.19	10.19	11.22	9.70	9.96	11.53	10.23	10.33	11.11	11.23	11.08
CH ₂ CHO	$^2A^{\prime\prime} \rightarrow {}^1A^{\prime}$	9.97	9.56	10.25	9.65	9.41	10.18	9.77	9.53	10.11	10.22	10.16
C_4O	$^3\Sigma^- \rightarrow {}^2\Pi$	9.52	9.19	9.56	9.03	8.96	9.69	9.42	9.23	9.41	9.78	9.63
BP	$^{3}\Pi \rightarrow {}^{4}\Sigma^{-}$	8.91	8.52	8.94	9.01	8.79	8.98	8.91	8.71	8.96	9.18	9.16
C_3H_5	$^2A_2 \rightarrow {}^1A_1$	7.94	7.51	8.09	7.43	7.07	7.91	7.56	7.22	7.82	8.05	7.98
N_3	$^{2}\Pi_{g} \rightarrow ^{3}\Sigma_{g}^{-}$	10.32	10.16	10.36	10.67	10.69	10.58	10.62	10.58	10.38	10.78	10.75
SCN	$^{2}\Pi \rightarrow ^{3}\Sigma^{-}$	10.09	9.88	10.24	10.09	9.96	10.37	10.27	10.08	10.36	10.45	10.41
CH_2CN	$^2B_1 \rightarrow {}^1A_1$	10.04	9.64	10.20	9.63	9.32	10.10	9.92	9.60	9.99	10.23	10.09
C_2H_3	$^2A' \rightarrow ^1A'$	9.64	9.17	9.84	9.22	8.77	9.66	9.39	8.92	9.64	9.72	9.61
CNN	$^3\Sigma^- \rightarrow {}^2\Pi$	11.31	10.93	11.36	10.80	10.51	11.25	10.94	10.54	11.24	11.40	11.17
C_3H_3	$^2B_1 \rightarrow {}^1A_1$	8.52	8.13	8.67	8.06	7.72	8.51	8.31	7.95	8.43	8.66	8.53
CH	$^{2}\Pi \rightarrow ^{1}\Sigma^{+}$	10.39	9.95	10.37	10.43	9.98	10.40	10.42	9.96	10.39	10.46	10.44
CHN_2	$^2A^{\prime\prime} \rightarrow {}^3A^{\prime\prime}$	9.10	8.76	9.44	9.54	9.42	9.62	9.55	9.29	9.57	9.76	9.74
HCCN	$^3A^{\prime\prime} \rightarrow {}^2A^{\prime}$	10.49	10.00	10.65	9.92	9.64	10.53	10.31	9.99	10.36	10.63	10.48
CN	$^{2}\Sigma^{+} \rightarrow {}^{1}\Sigma$	12.71	12.74	13.93	12.81	12.35	14.27	13.05	13.13	14.27	13.84	15.28
NS	$^{2}\Pi \rightarrow {}^{1}\Sigma^{+}$	8.53	8.18	8.91	7.72	7.69	8.94	8.34	8.06	8.72	8.79	8.70
SiC	$^{3}\Pi \rightarrow {}^{4}\Sigma^{-}$	8.28	7.98	8.23	8.56	8.41	8.54	8.35	8.11	8.49	8.68	8.73
CP	$^2\Sigma^+ \rightarrow {}^3\Pi$	10.45	10.13	10.39	10.75	10.62	10.49	10.66	10.53	10.42	10.78	10.74
MAE STDV		0.40 0.58	0.67 0.47	0.27 0.39	0.56 0.55	0.74 0.57	0.18 0.30	0.44 0.56	0.61 0.40	0.16 0.23	0.17 0.36	

sensitive to significant spin contamination in the UHF reference than EA-ADC.

We now turn our attention to the IP-ADC/UHF and IP-EOM-CCSD/UHF vertical ionization energies (IPs) of WSM and SSM presented in Tables IV and V, respectively. The MAE and STDV for each method computed relative to CCSD(T)/ROHF are depicted in Fig. 3. As for EA-ADC, the largest MAE out of all IP-ADC/UHF approximations is demonstrated by IP-ADC(2)-X. For WSM, IP-ADC(3)/UHF is by far the most accurate UHF-based IP-ADC method, with MAE (0.09 eV) smaller than that of IP-ADC(2)/UHF (0.44 eV) by more than a factor of four. Upon increasing spin contamination from WSM to SSM, the IP-ADC/UHF calculations show trends similar to those in the EA-ADC/UHF results. In particular, the MAE of IP-ADC(3)/UHF increases by a factor of three (from 0.09 to 0.27 eV), the IP-ADC(2)-X/UHF MAE grows by ~12%, while IP-ADC(2)/UHF shows a small reduction in MAE from 0.44 to 0.40 eV. All three IP-ADC/UHF methods also exhibit a very significant increase in STDV, indicating that the growth in UHF spin contamination has a detrimental effect on reliability of these methods. The IP-EOM-CCSD/UHF method is similar to IP-ADC(3)/UHF in accuracy for WSM, but it is significantly more accurate for SSM.

To investigate how the performance of EA/IP-ADC/UHF methods is affected by spin contamination (ΔS^2) in charged excited states, we computed the sum and average of ΔS^2 for WSM and SSM presented in Figs. 4 and 5 for EA and IP, respectively. The calculated ΔS^2 values for each molecule are tabulated in the supplementary material. For WSM, the ΔS^2 value of IP-ADC/UHF decreases with the increasing level of IP-ADC theory and is smaller than the ΔS^2 value in EA-ADC/UHF results. The IP-ADC/UHF excited-state spin contamination is similar to the ΔS^2 value in UHF reference (Table I) for all WSM, except for O_2 , S_2 , BO, and SO where the ΔS^2 value of IP-ADC/UHF is significantly larger. On the contrary, the excited-state ΔS^2 in EA-ADC/UHF grows with the increasing order of ADC approximation and is greater than the ground-state ΔS^2 from UHF for all WSM, with the exception of SiF. Upon transitioning from WSM to SSM, the average ΔS^2 increases from ~0.05 to ~0.3 a.u. for IP-ADC/UHF and from ~0.15 to ~0.34 a.u. for EA-ADC/UHF. In contrast to WSM, increasing the level of IP-ADC/UHF approximation for SSM



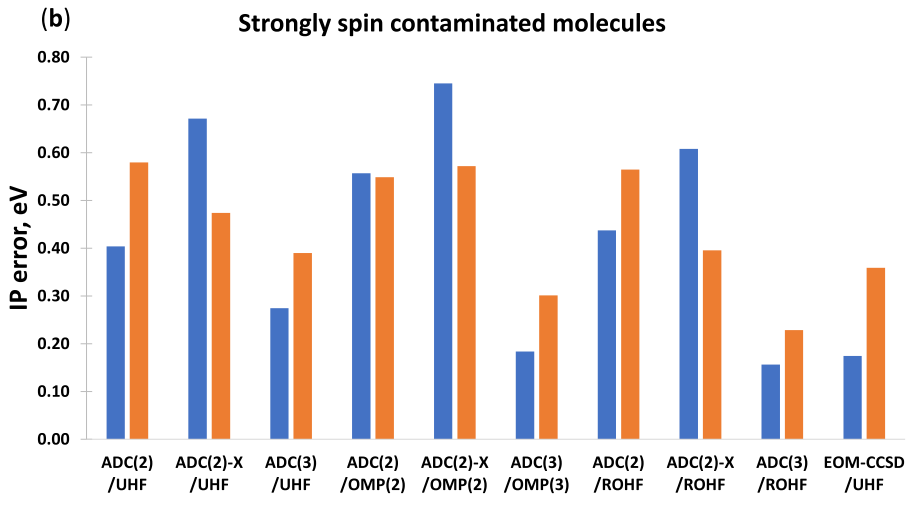


FIG. 3. Mean absolute errors (MAEs) and standard deviations (STDVs) in the IP-ADC vertical ionization energies (eV) for (a) 18 weakly and (b) 22 strongly spin-contaminated molecules with the ground-state UHF spin contamination of <0.1 and ≥0.1 a.u., respectively. Reference data are from CCSD(T). The aug-cc-pVDZ basis set was used. See Tables IV and V for data on individual molecules.

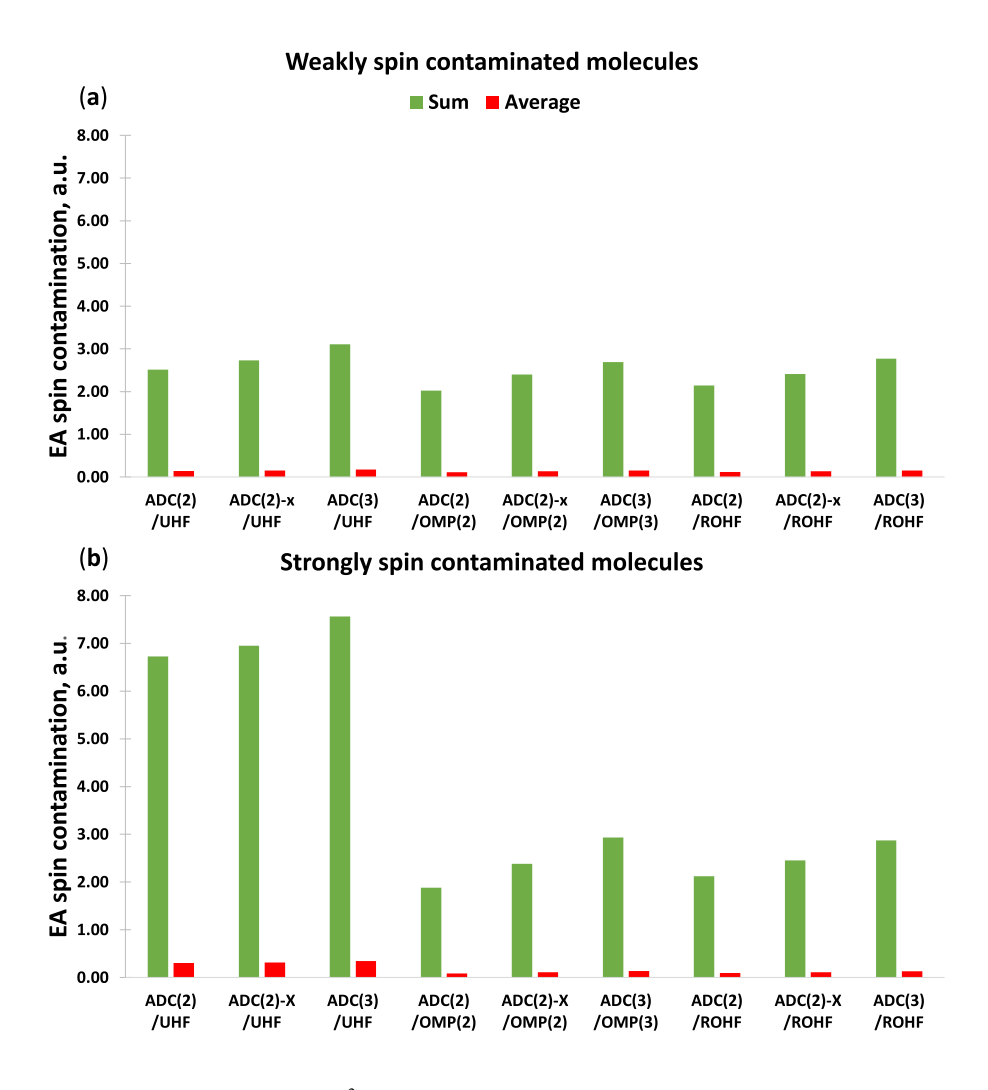


FIG. 4. Sum and average of spin contamination in the lowest-energy electronattached state for (a) 18 weakly and (b) 22 strongly spin-contaminated molecules computed using EA-ADC with three different reference wavefunctions. The aug-cc-pVDZ basis set was used.

does not lower the average ΔS^2 , which remains relatively constant (~0.3 a.u.). The EA-ADC/UHF results of SSM show a substantial increase in total and average ΔS^2 from EA-ADC(2) to EA-ADC(3).

Overall, our results indicate that the increasing spin contamination in UHF reference significantly worsens the performance of EA/IP-ADC(2)-X/UHF and EA/IP-ADC(3)/UHF methods, while the accuracy of EA/IP-ADC(2)/UHF is affected much less. However, when the UHF wavefunction is strongly spin contaminated, charged excited states computed using all UHF-based ADC approximations exhibit a large spin contamination ($\Delta S^2 > 0.1~\text{a.u.}$). In Secs. IV B and IV C, we investigate how the performance of EA/IP-ADC approximations is affected by reducing the spin contamination in the reference wavefunction.

B. Reducing spin contamination using the orbital-optimized [OMP(n)] reference

Combining orbital optimization with conventional perturbation theories such as MP(n) (n=2,3) has been shown to significantly improve their accuracy for the open-shell molecules with significant spin contamination in the UHF reference wavefunction. ^{71,72,96,97,106} Table I demonstrates that incorporating

the orbital relaxation and electron correlation effects together in OMP(n) reduces the ground-state ΔS^2 to almost zero for all molecules studied in this work, while treating electron correlation with the UHF orbitals [MP(n)/UHF] has a much smaller effect on spin contamination, resulting in a large ΔS^2 for most SSM.

Figures 4 and 5 depict the sum and average of ΔS^2 in the lowest-energy charged states of WSM and SSM computed using EA/IP-ADC(n)/OMP(n). Optimizing the reference orbitals has a minor (~10%) effect on the average ΔS^2 for WSM, but it gives rise to a threefold reduction in the average ΔS^2 for SSM. The total and mean ΔS^2 values of electron-attached states computed using EA-ADC(n)/OMP(n) are similar for WSM and SSM at each order of perturbation theory, respectively (Fig. 4). For the ionized states, the average IP-ADC(n)/OMP(n) spin contamination for SSM remains significantly higher than that for WSM (Fig. 5).

Figure 3 illustrates that reducing the spin contamination in ground and excited states does not significantly affect the accuracy of IP-ADC for WSM (Table IV). For SSM, using the OMP(n) orbitals increases the MAE and STDV in IP-ADC(2) and IP-ADC(2)-X vertical ionization energies while significantly lowering these error metrics for IP-ADC(3) (Table V). The increase in

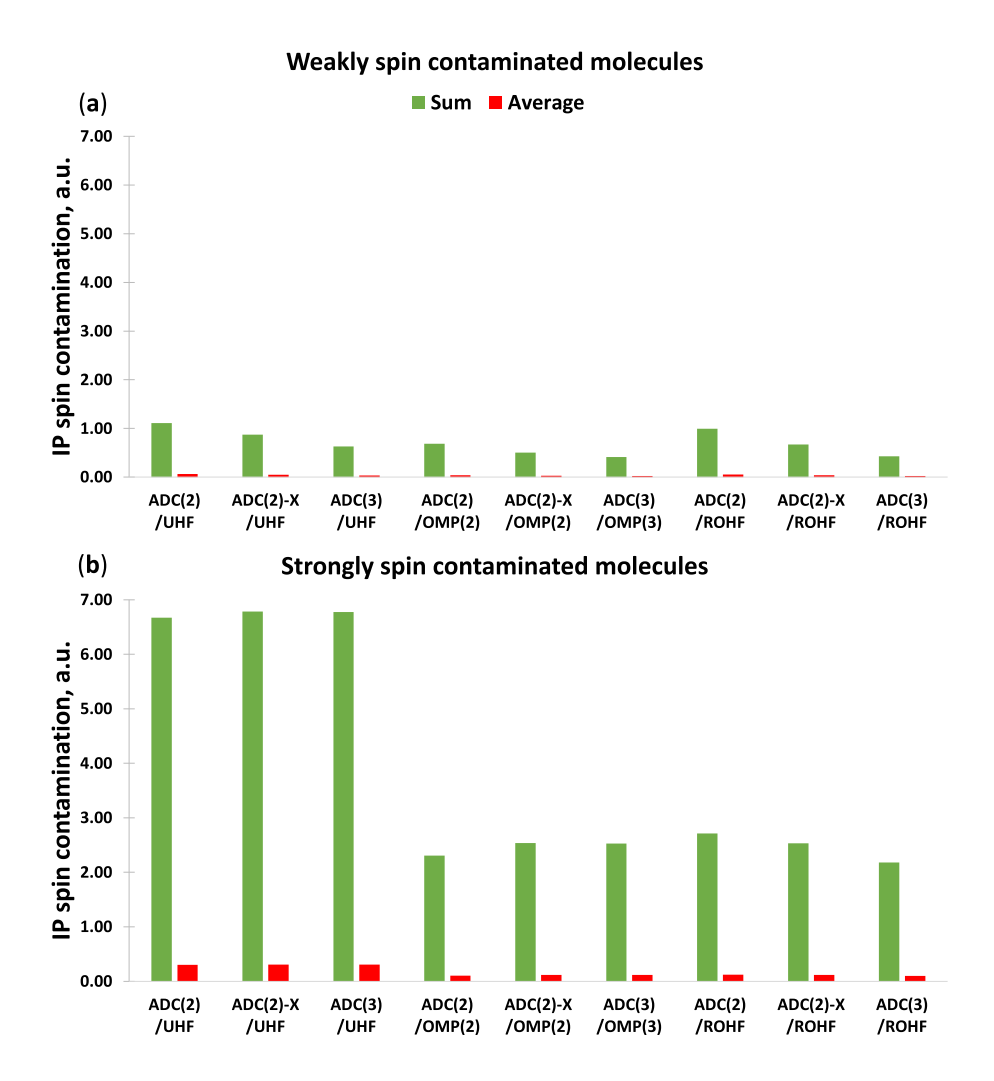


FIG. 5. Sum and average of spin contamination in the lowest-energy ionized state for (a) 18 weakly and (b) 22 strongly spin-contaminated molecules computed using IP-ADC with three different reference wavefunctions. The aug-cc-pVDZ basis set was used.

IP-ADC(2)/OMP(2) MAE relative to IP-ADC(2)/UHF suggests that the smaller MAE of the UHF-based method is a result of fortuitous error cancellation and that reducing the spin contamination in IP-ADC(2)/OMP(2) shifts the balance of error, worsening its performance. For both WSM and SSM, IP-ADC(3)/OMP(3) shows nearly the same MAE (0.18 eV) and smaller STDV (0.30 eV) relative to IP-EOM-CCSD/UHF, indicating that both methods are similarly accurate even for challenging open-shell molecules.

Similar trends are observed when comparing the errors in EA-ADC(n) vertical electron affinities computed using the UHF and OMP(n) reference orbitals, as illustrated in Fig. 2. Using the optimized orbitals does not significantly affect the accuracy of EA-ADC for WSM with the exception of EA-ADC(2)-X, which shows a large (\sim 0.3 eV) increase in MAE (Table II). When using an orbital-optimized reference for SSM, both EA-ADC(2) and EA-ADC(2)-X increase their MAE by \sim 75%–85% relative to the UHF-based methods (Table III). Optimizing the orbitals for EA-ADC(3) shows a significant (\sim 33%) reduction in the MAE for SSM that becomes nearly identical to that of EA-EOM-CCSD/UHF (0.17 eV). Importantly, these changes in the relative performance of EA-ADC(n)

methods for SSM restore the expected trend MAE [EA-ADC(2)] > MAE [EA-ADC(3)] that is not observed for the UHF reference.

To summarize, using the OMP(n) reference helps to substantially lower the spin contamination in charged excited states of SSM computed using EA/IP-ADC(n). The reduction in ΔS^2 significantly improves the performance of EA/IP-ADC(3), which show MAE and STDV similar to those of EA/IP-EOM-CCSD/UHF. In contrast, using the optimized orbitals affects the balance of error cancellation in EA/IP-ADC(2) and EA/IP-ADC(2)-X, increasing their errors.

C. Reducing spin contamination using the restricted open-shell (ROHF) reference

An alternative approach to reduce the spin contamination in post-Hartree–Fock calculations is to employ the ROHF reference (Sec. II D). We demonstrate this in Table I, which shows that the MP(n)/ROHF ground-state spin contamination is close to zero for most of the open-shell molecules considered in this work.

Figures 4 and 5 present the excited-state ΔS^2 computed using EA/IP-ADC/ROHF. As in Sec. IV B, the largest differences with the

EA/IP-ADC/UHF results are observed for SSM, where the ROHFbased EA/IP-ADC methods show much smaller excited-state spin contamination. The EA/IP-ADC with ROHF and OMP(n) references exhibit similar mean ΔS^2 , although the former reference tends to produce somewhat larger spin contamination, as reflected by the sum of ΔS^2 across the charged excited states of all molecules.

We now compare the performance of EA/IP-ADC methods with ROHF, OMP(n), and UHF references. The MAE and STDV of EA/IP-ADC(n)/ROHF are quite similar to those computed using EA/IP-ADC(n)/OMP(n) as illustrated in Figs. 2 and 3. Both ROHF and OMP(3) are equally effective in improving the accuracy of EA/IP-ADC(3) for SSM, with errors in vertical electron affinities and ionization energies similar to those from EA/IP-EOM-CCSD/UHF. When combined with EA/IP-ADC(2) and EA/IP-ADC(2)-X, the MAE produced by the ROHF reference tends to be smaller than those from OMP(2) by ~10%-20%. This reduction in error is correlated with somewhat higher spin contamination observed in the EA/IP-ADC(2)/ROHF and EA/IP-ADC(2)-X/ROHF calculations in comparison to those computed using the OMP(2) reference and can be attributed to error cancellation as described in Sec. IV B.

Overall, our results demonstrate that the ROHF reference is as effective as OMP(n) in reducing the excited-state spin contamination and the errors of EA/IP-ADC(3) approximations. At the EA/IP-ADC(2) and EA/IP-ADC(2)-X levels of theory, the ROHF calculations exhibit smaller errors compared to OMP(n), but they may suffer from somewhat higher spin contamination.

V. CONCLUSIONS

In this work, we investigated the effect of spin contamination on the performance of three single-reference ADC methods for the charged excitations of open-shell systems [EA/IP-ADC(2), EA/IP-ADC(2)-X, and EA/IP-ADC(3)]. To this end, we benchmarked the accuracy of EA/IP-ADC for 40 molecules with different levels of spin contamination in the unrestricted Hartree-Fock (UHF) reference wavefunction and developed an approach for calculating the expectation values of spin-squared operator and spin contamination in the EA/IP-ADC charged excited states. Our study demonstrates that the EA/IP-ADC results can be affected by significant spin contamination (ΔS^2), especially when ΔS^2 in the UHF reference wavefunction is large (≥0.1 a.u.). For such strongly spin-contaminated systems, the average errors of third-order ADC approximations [EA/IP-ADC(3)/UHF] increase by ~60% for EA and ~300% for IP, relative to molecules with the UHF $\Delta S^2 < 0.1$ a.u. The extended second-order methods [EA/IP-ADC(2)-X/UHF] also show significant increase (10%-15%) in their average errors upon increasing the spin contamination in UHF reference, while the accuracy of strict second-order approximations [EA/IP-ADC(2)/UHF] is affected much less.

To mitigate the spin contamination in ADC calculations, we implemented the EA/IP-ADC methods with reference orbitals from restricted open-shell Hartree-Fock (ROHF) and orbital-optimized *n*th-order Møller-Plesset perturbation [OMP(n)] theories. The results of our work provide clear evidence that the accuracy of EA/IP-ADC(3) is quite sensitive to the spin contamination in reference wavefunction. For strongly spin-contaminated open-shell molecules ($\Delta S^2 \ge 0.1$ a.u.), combining EA/IP-ADC(3) with ROHF or OMP(3) increases their accuracy by ~30%-50%. While both ROHF

and OMP(3) are equally effective in reducing spin contamination and improving the performance of EA/IP-ADC(3), the ROHF reference has a much lower computational scaling with the basis set size $[\mathcal{O}(N^4)]$ relative to that of OMP(3) $[\mathcal{O}(N^6)]$.

For EA/IP-ADC(2) and EA/IP-ADC(2)-X, using the ROHF or OMP(2) orbitals reduces the spin contamination in ground and excited electronic states of open-shell molecules, but increases the errors in vertical electron affinities and ionization energies. Although employing ROHF or OMP(2) leads to a significant loss in EA/IP-ADC(2) and EA/IP-ADC(2)-X accuracy for calculating the charged excitation energies, these reference wavefunctions may still be preferred over UHF if one is interested in calculating other excited-state properties that can be sensitive to spin contamination.

SUPPLEMENTARY MATERIAL

See the supplementary material for the working equations of EA/IP-ADC(n) with the ROHF reference, equations for the oneand two-particle density matrices, Cartesian geometries of 40 neutral open-shell molecules, and excited-state spin contamination and spectroscopic factors computed using all ADC methods.

ACKNOWLEDGMENTS

This work was supported by the start-up funds from the Ohio State University and by the National Science Foundation, under Grant No. CHE-2044648. Additionally, S.B. was supported by a fellowship from Molecular Sciences Software Institute under NSF Grant No. ACI-1547580. Computations were performed at the Ohio Supercomputer Center under Project Nos. PAS1583 and PAS1963.¹⁰⁷ The authors thank Ruojing Peng for contributions in the initial stage of this project.

AUTHOR DECLARATIONS

Conflict of Interest

The authors have no conflicts to disclose.

Author Contributions

Terrence L. Stahl: Data curation (equal); Investigation (equal); Software (equal); Visualization (equal); Writing - original draft (equal). Samragni Banerjee: Software (equal). Alexander Yu. Sokolov: Conceptualization (equal); Formal analysis (equal); Funding acquisition (equal); Project administration (equal); Resources (equal); Software (equal); Writing – review & editing (equal).

DATA AVAILABILITY

The data that support the findings of this study are available within the article and its supplementary material and from the corresponding author upon reasonable request.

REFERENCES

¹K. Seki, Mol. Cryst. Liq. Cryst. Incorporating Nonlinear Opt. 171, 255 (1989).

² J. Li, G. D'Avino, I. Duchemin, D. Beljonne, and X. Blase, Phys. Rev. B **97**, 035108

- ³B. W. D'Andrade, S. Datta, S. R. Forrest, P. Djurovich, E. Polikarpov, and M. E. Thompson, Org. Electron. **6**, 11 (2005).
- ⁴J. P. Perdew, W. Yang, K. Burke, Z. Yang, E. K. U. Gross, M. Scheffler, G. E. Scuseria, T. M. Henderson, I. Y. Zhang, A. Ruzsinszky *et al.*, Proc. Natl. Acad. Sci. U. S. A. 114, 2801 (2017).
- ⁵ A. Dittmer, R. Izsák, F. Neese, and D. Maganas, Inorg. Chem. **58**, 9303 (2019).
- ⁶D. Tripathi and A. K. Dutta, J. Phys. Chem. A **123**, 10131 (2019).
- ⁷D. M. Schultz and T. P. Yoon, Science **343**, 1239176 (2014).
- ⁸T. J. Wallington, M. D. Hurley, J. M. Fracheboud, J. J. Orlando, G. S. Tyndall, J. Sehested, T. E. Møgelberg, and O. J. Nielsen, J. Phys. Chem. **100**, 18116 (1996).
- ⁹S. Aloisio and J. S. Francisco, Acc. Chem. Res. 33, 825 (2000).
- ¹⁰G. S. Tyndall, R. A. Cox, C. Granier, R. Lesclaux, G. K. Moortgat, M. J. Pilling, A. R. Ravishankara, and T. J. Wallington, J. Geophys. Res.: Atmos. **106**, 12157, https://doi.org/10.1029/2000jd900746 (2001).
- ¹¹D. R. Glowacki and M. J. Pilling, ChemPhysChem 11, 3836 (2010).
- ¹²B. S. Narendrapurapu, A. C. Simmonett, H. F. Schaefer III, J. A. Miller, and S. J. Klippenstein, J. Phys. Chem. A 115, 14209 (2011).
- ¹³X. Sun, C. Zhang, Y. Zhao, J. Bai, Q. Zhang, and W. Wang, Environ. Sci. Technol. 46, 8148 (2012).
- ¹⁴M. Ramaiah, Tetrahedron **43**, 3541 (1987).
- ¹⁵M. P. Bertrand, Org. Prep. Proced. Int. 26, 257 (1994).
- 16 F. Dénès, M. Pichowicz, G. Povie, and P. Renaud, Chem. Rev. 114, 2587 (2014).
- ¹⁷ A. Khamrai and V. Ganesh, J. Chem. Sci. **133**, 5 (2021).
- 18 J. Lee, S. Hong, Y. Heo, H. Kang, and M. Kim, Dalton Trans. $\bf 50$, 14081 (2021).
- ¹⁹T. D. Crawford and H. F. Schaefer, Rev. Comput. Chem. 14, 33 (2000).
- ²⁰I. Shavitt and R. J. Bartlett, Many-Body Methods in Chemistry and Physics (Cambridge University Press, Cambridge, UK, 2009).
- ²¹ M. Nooijen and J. G. Snijders, Int. J. Quantum Chem. 44, 55 (1992).
- ²²J. F. Stanton and R. J. Bartlett, J. Chem. Phys. **98**, 7029 (1993).
- ²³M. Nooijen and J. G. Snijders, Int. J. Quantum Chem. 48, 15 (1993).
- ²⁴M. Nooijen and J. G. Snijders, J. Chem. Phys. **102**, 1681 (1995).
- ²⁵ A. I. Krylov, Annu. Rev. Phys. Chem. **59**, 433 (2008).
- ²⁶G. E. Scuseria and H. F. Schaefer, Chem. Phys. Lett. **142**, 354 (1987).
- ²⁷ A. I. Krylov, C. D. Sherrill, E. F. C. Byrd, and M. Head-Gordon, J. Chem. Phys. 109, 10669 (1998).
- ²⁸C. D. Sherrill, A. I. Krylov, E. F. C. Byrd, and M. Head-Gordon, J. Chem. Phys. 109, 4171 (1998).
- ²⁹ S. R. Gwaltney, C. D. Sherrill, M. Head-Gordon, and A. I. Krylov, J. Chem. Phys. 113, 3548 (2000).
- ³⁰R. C. Lochan and M. Head-Gordon, J. Chem. Phys. **126**, 164101 (2007).
- ³¹ U. Bozkaya, J. Chem. Phys. **135**, 224103 (2011).
- ³²U. Bozkaya, J. M. Turney, Y. Yamaguchi, H. F. Schaefer III, and C. D. Sherrill, J. Chem. Phys. **135**, 104103 (2011).
- ³³U. Bozkaya and C. D. Sherrill, J. Chem. Phys. **138**, 184103 (2013).
- 34 U. Bozkaya, J. Chem. Phys. 139, 104116 (2013).
- 35 U. Bozkaya and H. F. Schaefer III, J. Chem. Phys. 136, 204114 (2012).
- ³⁶U. Bozkaya and C. D. Sherrill, J. Chem. Phys. **139**, 054104 (2013).
- ³⁷ A. Y. Sokolov, A. C. Simmonett, and H. F. Schaefer, J. Chem. Phys. 138, 024107 (2013).
- 38 R. J. Buenker and S. D. Peyerimhoff, Theor. Chim. Acta 35, 33 (1974).
- ³⁹ P. E. M. Siegbahn, J. Chem. Phys. **72**, 1647 (1980).
- ⁴⁰H. J. Werner and P. J. Knowles, J. Chem. Phys. **89**, 5803 (1988).
- ⁴¹D. Mukherjee, R. K. Moitra, and A. Mukhopadhyay, Mol. Phys. 33, 955 (1977).
- ⁴²F. A. Evangelista, W. D. Allen, and H. F. Schaefer, J. Chem. Phys. **127**, 024102 (2007).
- ⁴³D. Datta, L. Kong, and M. Nooijen, J. Chem. Phys. **134**, 214116 (2011).
- ⁴⁴A. Köhn, M. Hanauer, L. A. Mück, T.-C. Jagau, and J. Gauss, Wiley Interdiscip. Rev.: Comput. Mol. Sci. **3**, 176 (2013).
- ⁴⁵D. Datta and M. Nooijen, J. Chem. Phys. **137**, 204107 (2012).
- ⁴⁶ A. Banerjee, R. Shepard, and J. Simons, Int. J. Quantum Chem. 14, 389 (1978).
- ⁴⁷J. A. Nichols, D. L. Yeager, and P. Jørgensen, J. Chem. Phys. **80**, 293 (1984).
- ⁴⁸V. F. Khrustov and D. E. Kostychev, Int. J. Quantum Chem. 88, 507 (2002).
- ⁴⁹ K. Chatterjee and A. Y. Sokolov, J. Chem. Theory Comput. **15**, 5908 (2019).

- ⁵⁰ K. Chatterjee and A. Y. Sokolov, J. Chem. Theory Comput. 16, 6343 (2020).
- ⁵¹ C. E. V. de Moura and A. Y. Sokolov, *Phys. Chem. Chem. Phys.* **24**, 4769 (2022).
- ⁵² J. Schirmer, Phys. Rev. A **26**, 2395 (1982).
- ⁵³ J. Schirmer, Phys. Rev. A **43**, 4647 (1991).
- ⁵⁴F. Mertins and J. Schirmer, Phys. Rev. A **53**, 2140 (1996).
- ⁵⁵ J. Schirmer and A. B. Trofimov, J. Chem. Phys. **120**, 11449 (2004).
- ⁵⁶A. Dreuw and M. Wormit, Wiley Interdiscip. Rev.: Comput. Mol. Sci. 5, 82 (2014).
- ⁵⁷J. Schirmer, L. S. Cederbaum, and O. Walter, Phys. Rev. A **28**, 1237 (1983).
- ⁵⁸J. Schirmer, A. B. Trofimov, and G. Stelter, J. Chem. Phys. **109**, 4734 (1998).
- ⁵⁹ A. B. Trofimov and J. Schirmer, J. Chem. Phys. **123**, 144115 (2005).
- ⁶⁰ A. B. Trofimov and J. Schirmer, in *Proceedings of 14th European Symposium on Gas Phase Electron Diffraction* (Moscow State University, 2011), p. 77.
- ⁶¹ M. Schneider, D. Y. Soshnikov, D. M. P. Holland, I. Powis, E. Antonsson, M. Patanen, C. Nicolas, C. Miron, M. Wormit, A. Dreuw, and A. B. Trofimov, J. Chem. Phys. 143, 144103 (2015).
- ⁶² A. L. Dempwolff, M. Schneider, M. Hodecker, and A. Dreuw, J. Chem. Phys. 150, 064108 (2019).
- ⁶³S. Banerjee and A. Y. Sokolov, J. Chem. Phys. **151**, 224112 (2019).
- ⁶⁴ A. L. Dempwolff, A. C. Paul, A. M. Belogolova, A. B. Trofimov, and A. Dreuw, J. Chem. Phys. **152**, 024113 (2020).
- ⁶⁵ A. L. Dempwolff, A. C. Paul, A. M. Belogolova, A. B. Trofimov, and A. Dreuw, J. Chem. Phys. **152**, 024125 (2020).
- ⁶⁶J. Liu, C. Hättig, and S. Höfener, J. Chem. Phys. **152**, 174109 (2020).
- ⁶⁷S. Banerjee and A. Y. Sokolov, J. Chem. Phys. **154**, 074105 (2021).
- ⁶⁸ A. L. Dempwolff, A. M. Belogolova, A. B. Trofimov, and A. Dreuw, J. Chem. Phys. **154**, 104117 (2021).
- ⁶⁹C. C. J. Roothaan, Rev. Mod. Phys. **32**, 179 (1960).
- ⁷⁰ J. Lee and M. Head-Gordon, J. Chem. Phys. **150**, 244106 (2019).
- ⁷¹L. W. Bertels, J. Lee, and M. Head-Gordon, J. Phys. Chem. Lett. **10**, 4170 (2019).
- ⁷²F. Neese, T. Schwabe, S. Kossmann, B. Schirmer, and S. Grimme, J. Chem. Theory Comput. 5, 3060 (2009).
- 73 W. Kurlancheek and M. Head-Gordon, Mol. Phys. 107, 1223 (2009).
- ⁷⁴ A. L. Fetter and J. D. Walecka, Quantum Theory of Many-Particle Systems (Dover Publications, 2003).
- ⁷⁵W. H. Dickhoff and D. Van Neck, Many-Body Theory Exposed!: Propagator Description of Quantum Mechanics in Many-Body Systems (World Scientific Publishing Co., 2005).
- ⁷⁶D. Danovich, Wiley Interdiscip. Rev.: Comput. Mol. Sci. 1, 377 (2011).
- ⁷⁷ A. B. Trofimov, G. Stelter, and J. Schirmer, J. Chem. Phys. 111, 9982 (1999).
- ⁷⁸ M. D. Prasad, S. Pal, and D. Mukherjee, *Phys. Rev. A* 31, 1287 (1985).
- ⁷⁹D. Mukherjee and W. Kutzelnigg, Many-Body Methods in Quantum Chemistry (Springer, Berlin, Heidelberg, 1989), pp. 257–274.
- ⁸⁰ A. Y. Sokolov, J. Chem. Phys. **149**, 204113 (2018).
- ⁸¹ I. M. Mazin and A. Y. Sokolov, J. Chem. Theory Comput. **17**, 6152 (2021).
- 82 C. Møller and M. S. Plesset, Phys. Rev. 46, 618 (1934).
- ⁸³ M. Hodecker, A. L. Dempwolff, J. Schirmer, and A. Dreuw, J. Chem. Phys. 156, 074104 (2022).
- ⁸⁴D. Stück and M. Head-Gordon, J. Chem. Phys. **139**, 244109 (2013).
- ⁸⁵J. S. Andrews, D. Jayatilaka, R. G. A. Bone, N. C. Handy, and R. D. Amos, Chem. Phys. Lett. **183**, 423 (1991).
- ⁸⁶ A. I. Krylov, Rev. Comput. Chem. **30**, 151 (2017).
- ⁸⁷ M.-P. Kitsaras and S. Stopkowicz, J. Chem. Phys. **154**, 131101 (2021).
- ⁸⁸ J. Kouba and Y. Öhrn, Int. J. Quantum Chem. **3**, 513 (1969).
- ⁸⁹G. D. Purvis, H. Sekino, and R. J. Bartlett, Collect. Czech. Chem. Commun. 53, 2203 (1988).
- 90 J. F. Stanton, J. Chem. Phys. 101, 371 (1994).
- ⁹¹ A. I. Krylov, J. Chem. Phys. 113, 6052 (2000).
- ⁹²S. Knippenberg, D. R. Rehn, M. Wormit, J. H. Starcke, I. L. Rusakova, A. B. Trofimov, and A. Dreuw, J. Chem. Phys. **136**, 064107 (2012).
- 93 F. Plasser, M. Wormit, and A. Dreuw, J. Chem. Phys. 141, 024106 (2014).
- ⁹⁴ F. Plasser, S. A. Bäppler, M. Wormit, and A. Dreuw, J. Chem. Phys. **141**, 024107 (2014).

- ⁹⁵ P. J. Knowles, J. S. Andrews, R. D. Amos, N. C. Handy, and J. A. Pople, Chem. Phys. Lett. **186**, 130 (1991).
- ⁹⁶U. Bozkaya, J. Chem. Theory Comput. **10**, 4389 (2014).
- ⁹⁷E. Soydaş and U. Bozkaya, J. Chem. Theory Comput. 11, 1564 (2015).
- ⁹⁸ Q. Sun, X. Zhang, S. Banerjee, P. Bao, M. Barbry, N. S. Blunt, N. A. Bogdanov, G. H. Booth, J. Chen, Z.-H. Cui *et al.*, J. Chem. Phys. **153**, 024109 (2020).
- ⁹⁹ E. Epifanovsky, A. T. B. Gilbert, X. Feng, J. Lee, Y. Mao, N. Mardirossian, P. Pokhilko, A. F. White, M. P. Coons, A. L. Dempwolff *et al.*, J. Chem. Phys. 155, 084801 (2021).
- ¹⁰⁰ J. D. Watts, J. Gauss, and R. J. Bartlett, J. Chem. Phys. 98, 8718 (1993).

- ¹⁰¹ K. Raghavachari, G. W. Trucks, J. A. Pople, and M. Head-Gordon, Chem. Phys. Lett. 157, 479 (1989).
- ¹⁰²R. J. Bartlett, J. D. Watts, S. A. Kucharski, and J. Noga, Chem. Phys. Lett. **165**, 513 (1990).
- ¹⁰³T. H. Dunning, Jr., J. Chem. Phys. **90**, 1007 (1989).
- ¹⁰⁴Y. Shao, Z. Gan, E. Epifanovsky, A. T. B. Gilbert, M. Wormit, J. Kussmann, A. W. Lange, A. Behn, J. Deng, X. Feng et al., Mol. Phys. 113, 184 (2015).
- 105 D. A. Matthews, L. Cheng, M. E. Harding, F. Lipparini, S. Stopkowicz, T.-C. Jagau, P. G. Szalay, J. Gauss, and J. F. Stanton, J. Chem. Phys. 152, 214108 (2020).
 106 E. Soydaş and U. Bozkaya, J. Chem. Theory Comput. 9, 1452 (2013).
- 107 See http://osc.edu/ark:/19495/f5s1ph73 for Ohio Supercomputer Center.